12

On the Relationship Between Boundary Layer Convergence and Cloud-to-Ground Lightning

Michael L. Gauthier*
United States Air Force Academy
USA

1. Introduction

It is generally accepted that significant electrification, and subsequent lightning generation, in clouds is attained via non-inductive charging (NIC) when sufficient numbers of ice crystals collide with graupel particles in the presence of supercooled liquid water [e.g. Saunders et al., 1991; Jayaratne et al., 1983; Takahashi, 1978]. As these particle scale interactions are driven by vertical motions it can be argued that, under appropriate thermodynamical and microphysical conditions, any process that enhances updraft strength should also enhance the storms ability to generate lightning.

Constrained by mass continuity, updrafts leading to deep moist convection are necessarily associated with sub-cloud horizontal mass convergence. Given that the Earth's surface is impermeable with respect to the wind, it is clear that horizontal convergence of boundary layer winds should result in compensating upward vertical motions with greater convergence over a given area resulting in greater vertical motions, possibly capable of initiating and/or intensifying convection. All else being equal (i.e., sufficient moisture and instability requisite for the development of deep moist convection), enhancements in boundary layer convergence (BLC) should deepen the planetary boundary layer (PBL), thereby enhancing the instability, with the end result being an increase in the number of updrafts capable of breaking the "cap" (capping inversion) allowing for more vigorous interactions between precipitation sized ice particles and ascending ice crystals within the charging zone, ultimately resulting in enhancements in thunderstorm electrification and lightning via NIC.

The effect of enhanced BLC, and the atmospheric response (i.e., rainfall and/or lightning) has been illustrated in previous observational studies from southern Florida [Ulanski and Garstang, 1978; Watson and Blanchard, 1984; Watson et al., 1987], highlighting the importance that boundary layer winds have on new thunderstorm growth and potential lightning production. In particular, Watson and Blanchard [1984], examined 121 convergence "events" during the 1975 Florida Area Cumulus Experiment (FACE) campaign and found a relationship between the change in total area divergence (the negative of which is used in this study; total area convergence (TAC), discussed in Section 3.3) and the amount

* The views expressed in this paper are those of the author and do not reflect the official policy or position of the U.S. Air Force, Department of Defense or the U.S. Government.

of radar-derived rainfall. Watson et al. [1987] coupled these findings with those that documented a proportionality between thunderstorm precipitation output and the total number of flashes [i.e., Workman and Reynolds, 1949; Battan, 1965], by relating cloud-to-ground (CG) lightning with surface wind convergence (both spatially and temporally) for 42 summer days in 1983 over central Florida. Their examination of divergence and lightning time series during this period showed that CG lightning began near the time of strongest convergence, peak lightning activity typically occurred when the total area divergence was near zero in the transition from convergence to divergence, and CG lightning ended just after peak divergence over the area. Further, through a set of scaling arguments Banacos and Schultz [2005] showed that horizontal mass convergence associated with smaller mesoscale boundaries such as lake/sea breezes, and active or remnant convective outflow boundaries, is at least an order of magnitude larger [$O(10^{-4}s^{-1})$] than convergence associated with typical frontal boundaries.

More recently, Gauthier [*in press*] found that, from a climatological sense, urban heat island (UHI) thermodynamics not only provided a more favorable environment for convection over the Houston area, but that the UHI acts to enhance the inland progression of the sea-breeze, thereby creating an enhanced area of localized convergence over the northern central portion of the city. The author then went on to assert that the spatial extent of the flash density features in and around the Houston area (to be described in Section 2.1) were "primarily the result of typical convective activity tied to the presence of a persistent thermal anomaly over the center of the city, giving rise to a preferential location of low-level convergence and convective enhancement."

Utilizing boundary layer convergence fields generated by the National Center for Atmospheric Research's (NCAR) Variational Doppler Radar Assimilation System (VDRAS; [Sun and Crook, 1997]), this study complements previous lightning [Gauthier et al., 2005], radar [Gauthier et al., 2006] and convergence [Gauthier, *in press*] climatologies presented in the literature, independently establishing the presence of an enhanced convergence zone located in the vicinity of the Houston metropolitan area, generally co-located with the observed climatological enhancement in cloud-to-ground lightning over and downwind of the city. Area averaged, and cell-scale analyses link boundary layer convergence (forcing #1) with enhancements in radar derived precipitation ice mass (response #1, forcing #2) and ultimately enhanced ground flash densities (response #2).

2. Background

2.1 Houston and the Houston lightning anomaly

An area lacking significant orographic features, Houston sits adjacent to the complex coastline of Galveston Bay (to the southeast) with over 50 km^2 of winding and stationary waterways dispersed throughout. In addition to the Houston shipping channel, a heavily industrialized link between the city and the Gulf of Mexico, there are four major bayous that transect the city, with Lake Houston, a significant ground-level water source located approximately 30 km to the northeast of city center. The climate of Houston is classified as humid subtropical, with its proximity to Galveston Bay and the Gulf of Mexico causing winters to be quite mild, while the summers are rather hot and humid. Summer air temperatures average 33^o C (92^o F) during the day and 23^o C (73^o F) at night with mean daily

dewpoint temperatures of 22° C (72° F). Southerly winds prevail during the summer months with wind speeds averaging 4 m s^{-1}, with an average of 19 lightning days per summer [Gauthier et al., 2005].

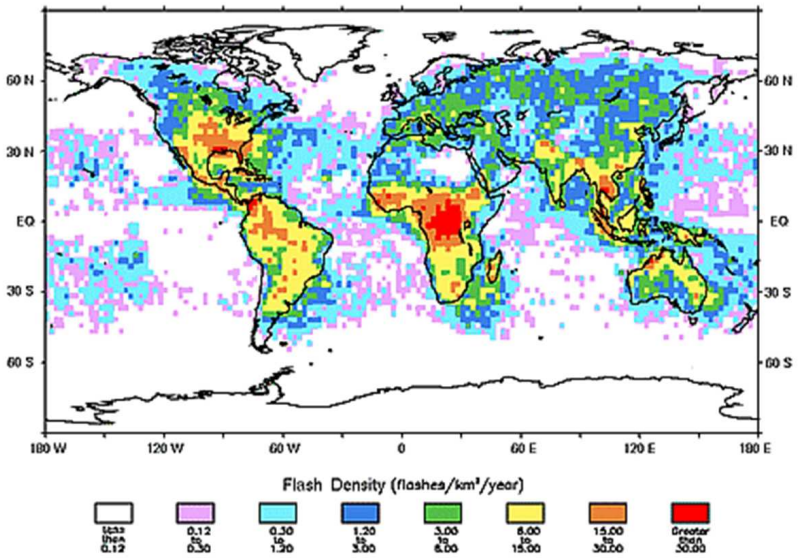

Fig. 1. Spatial distribution of annual global lightning activity between September 1, 1995 and August 31, 1996 as observed by NASA's OTD. Lightning flash densities (flashes km^{-2} $year^{-1}$) were calculated statistically using OTD data from more than 400 separate 3-minute observations of each location on the earth (SOURCE: http://thunder.msfc.nasa.gov/otd/).

Using 12-years of CG lightning data (1989-2000) gathered by the NLDN, Orville et al. [2001] documented a persistent, year-round, enhancement in CG lightning activity downwind of the Houston metropolitan area. Steiger et al. [2002], using the same data set (5 km spatial resolution), quantified the enhancement observed by Orville et al., reporting a 45% increase in annual CG lightning flash densities over and downwind of the Houston urban corridor relative to rural surroundings. Their findings are generally consistent with previous studies [i.e., Westcott, 1995], indicating that observed enhancements in CG flash densities can occur over, and downwind of urban corridors. To further study this documented lightning anomaly, Gauthier et al. [2005] performed an independent analysis on an extended subset of the CG lightning dataset (1995 – 2003) referenced in the literature [Orville et al., 2001; Steiger et al., 2002]. Their findings indicate that the local Houston CG lightning anomaly is a persistent summer-season feature (even when large lightning events were excluded from the analysis), with flash densities over and downwind of the Houston metropolitan area approaching 1.5-2 times that of immediate surroundings. However, when examined more regionally, they found the feature to be statistically non-unique, embedded with "anomalies" of similar scale within the more general enhancement of CG lightning along the Texas and Louisiana Gulf Coast. In fact, examination of annual lightning flash densities (flashes km^{-2} $year^{-1}$; Figure 1) observed by NASA's Optical Transient Detector (OTD) reveals a broad region of coastal enhancements, situated along the central Gulf of Mexico (including

the Houston area), in *total*, not just CG lightning activity. This indicates that the Houston area likely falls victim to enhanced intra-cloud lightning activity as well.

2.2 Thunderstorm electrification – The physics of the problem

Although the exact processes by which thunderstorms become electrified and ultimately lower charge to the surface of the Earth is still debated, it is generally accepted that significant electrification, and subsequent lightning generation, in clouds is attained via NIC when sufficient numbers of ice crystals collide with graupel particles in the presence of supercooled liquid water [e.g. Saunders et al., 1991; Jayaratne et al., 1983; Takahashi, 1978]. Here, as graupel particles grow in the mixed-phase region of a developing storm, suspended by convective updrafts, smaller ice crystals are swept past the graupel and subsequently transported into the upper portions of the storm. Rebounding collisions between the graupel particles and ice crystals result in negative charge being deposited on the graupel particles, and positive charge being deposited on the ice crystals. This process leads to the development of an electrical dipole, with positive charge situated over negative charge. Once the graupel's terminal velocity exceeds the storm updraft speed, it will begin to fall towards the surface of the Earth. Graupel/ice collisions occurring below the charge reversal temperature, which is some threshold between –5^{O}C and –10^{O}C dependent on liquid water content (LWC), will result in the falling graupel particles becoming positively charged and the ascending ice crystals negatively charged. The rising ice crystals can contribute to the elevated negative charge region, while the descending graupel particles produce a small positive charge region below the main negative charge center. The result is the development of an electrical tripole (with the negative charge region sandwiched between two positive charge regions) in agreement with observed tripoles structure in typical thunderstorms [Williams, 1989].

While the tripole model just described is conveniently simple, it is important to note that there remains considerable complexity in the microphysical charge separation process, and not all thunderstorms ascribe to this simple model. However, the larger-scale physics associated with the NIC mechanism remain valid, with three key requirements for thunderstorm electrification and subsequent lightning production: (1) the existence of convective updrafts, capable of (2) suspending precipitation ice mass in the mixed-phase region of the storm, allowing (3) rebounding graupel-ice crystal collisions to occur. Although these requisite ingredients are critical to the thunderstorm electrification process, it is clear that (2) and (3) can not occur without the presence of a significant convective updraft, with stronger updrafts capable of producing more lightning with increased ground flash densities.

From the above discussions it is readily apparent that the occurrence of lightning should be correlated to updraft strength (which ultimately allows for mixed phase interactions between graupel particles and ice crystals). Therefore, under the appropriate thermodynamical and microphysical conditions, any process that enhances updraft strength should also enhance the storms ability to generate lightning. Given that the Earth's surface is impermeable with respect to the wind, it is clear that horizontal convergence of the winds occurring within the boundary layer will result in compensating vertical motions with greater convergence over a given area resulting in greater vertical motions. These convergence based vertical motions, if co-located with existing updrafts, can enhance

updraft intensity which, given the underlying physics of the problem, should ultimately lead to enhancements in thunderstorm electrification.

As previously mentioned in Section 1, Gauthier [*in press*] found the spatial extent of the flash density features over the Houston area to be primarily the result of "typical" convective activity tied to the presence of a persistent thermal anomaly over the center of the city. This persistent thermal anomaly, coupled with the land surface heterogeneity of the surrounding area, gives rise to a preferential location of low-level convergence and convective enhancement. They concluded that, from a climatic viewpoint, the primary causative mechanisms responsible for the *intensity* of the Houston CG lightning anomaly (i.e., *those responsible for the predominant enhancements to the background, "typical",* features just described) to be those that serve to enhance low-level convergence; specifically that UHI thermodynamics contribute to an area of preferred convergence over, and to the east-northeast of the city, while also driving *mesoscale enhancements in sea breeze convergence*. Acting together, these two enhancements are argued to cause more frequent convection over the Houston urban area resulting in more lightning activity over the city.

2.3 VDRAS – Diagnosing convergence in the boundary layer

As VDRAS is an analysis tool developed, maintained and operated by NCAR, and the intent of this study it to evaluate the relationship between boundary layer convergence (as diagnosed by VDRAS), radar derived precipitation ice mass, and lightning, this section provides the reader with a cursory overview of VDRAS. For a detailed description of the system the reader is referred to Sun and Crook [1997], Sun and Crook [1998] and Crook and Sun [2001].

It has long been recognized that the success of numerical weather prediction (NWP) models depends strongly on the accuracy with which the atmosphere is represented at the time of model initialization. Unfortunately, by themselves, traditional weather observations provide a less than complete dataset from which to describe the initial state of the atmosphere in these models. Herein lies the need to incorporate, or assimilate, "unconventional" sources of weather information such as in-situ measurements and/or satellite observed/derived quantities into atmospheric NWP models to help "fill the gaps" in traditional observing networks, and provide a more complete (and hopefully more accurate) description of the atmosphere for use in the critical model initialization process. As its name implies, VDRAS utilizes a four-dimensional variational assimilation technique to incorporate a time series of radar observations (both radial velocity and reflectivity) from WSR-88D radars into a cloud-scale numerical model in order to better represent the evolution of flow (components of the horizontal wind) within the atmosphere. Through the minimization of a cost function, the model is fit to the observations over a specified period of time in order to develop a set of optimal initial conditions for use by the constraining numerical model.

VDRAS has been applied in both research and operational environments; the application of the system to different stages of convective development has demonstrated that the detailed structure of wind, thermodynamics and microphysics could be obtained with reasonable accuracy [Sun and Crook, 1998; Sun and Crook, 2001], thereby highlighting the utility of the system in diagnosing convergence within the boundary layer. Application of VDRAS generated fields to lightning studies such as this is a new endeavor; therefore, the

work presented here can be considered a *"first of its kind"* [A. Crook, personal communications, 2005].

3. Data and method

This study complements previous datasets (CG lightning, radar reflectivity, and precipitation ice mass) used by the author to investigate the documented enhancement in cloud-to-ground lightning over, and downwind of, the Houston metropolitan area by incorporating BLC fields through the assimilation of radial velocity data contained within the radar reflectivity dataset used by Gauthier et al. [2006] (described in Section 3.1) into VDRAS. Data gathered were used to construct a spatial climatology of convergence throughout the domain, with accompanying area and cell-scale analyses used to investigate the relationship between BLC, precipitation ice mass (IM) and CG flash densities and counts (FD and FC, respectively).

Two separate analysis methods were used to compare warm-season statistics of VDRAS derived BLC, radar derived IM, and NLDN detected FDs and FCs, both of which mimic the approach used by Gauthier et al. [2006] where similar analyses were performed comparing IM with FDs and FCs. The first method compared time-integrated (TI) or cumulative means of BLC, IM and FD for each 4 km grid square within the domain yielding a total of 10,000 data points for comparison (one for each 16 km^2 pixel within the horizontal analysis domain). The second approach utilized the cell identification component of the Interactive Data Language (IDL) cell-tracking algorithm used by Gauthier et al. [2010] to compare storm integrated BLC values with storm IMs, FCs and FDs on a cell-by-cell basis (described in Section 3.4). Here, the original software was modified to incorporate the VDRAS BLC dataset. A total of 14,061 cells were identified and analyzed as part of this study.

3.1 Radar and CG lightning methodologies

Using the synoptically conditioned dataset from Gauthier [*in-press*], over 1,200 daytime (0900 – 1659 CST) convective volumes of archived WSR-88D Level II data [detailed in Gauthier et al., 2006] from 15 lightning days over Houston were selected for assimilation into VDRAS. In addition to the requirement for the occurrence of at least one CG lightning strike over the Houston area, included volumes occurred on days in which synoptic conditions were deemed favorable for the formation of a sea breeze circulation.

Radar data from each of these days were processed using two separate schemes, one for the VDRAS analysis performed at NCAR, and a second for the area and cell-scale analyses (conducted locally). In all instances the domain spanned 400 km x 400 km, centered on the location of the League City, TX radar site. For the VDRAS analyses, the Level II data were shipped to NCAR where they were interpolated to a 1 km Cartesian grid in the horizontal while an unfolding algorithm was applied to the radial velocity input data stream. Following gridding, the data underwent an automated quality control process, and was then further interpolated onto the 4 km model grid in the horizontal while remaining on the constant elevation angle levels in the vertical. The vertical resolution of the VDRAS output grids were 0.5 km, extending to an altitude of 7 km. Radar data was also locally gridded so that radar derived precipitation ice mass quantities could be calculated [as detailed by Gauthier et al., 2006] with horizontal resolutions matching that of the VDRAS grid; vertical

resolution was 1 km, extending 20 km in the vertical to allow for computation of precipitation ice mass quantities throughout the domain.

Coincident with each radar volume, ground strike locations (i.e., flashes occurring from the beginning of one volume scan to the beginning of the subsequent volume scan) detected by the NLDN were gridded to match the horizontal dimensions of the Cartesian VDRAS and radar grids. For consistency, positive ground flashes with peak currents less than 10 kA have been disregarded [c.f., Cummins et al., 1998; Wacker and Orville, 1999a, b; Gauthier et al., 2005].

3.2 VDRAS methodology

The assimilation window for VDRAS is 10 minutes, meaning that a total of three consecutive volumes of radar data (constant elevation levels) were used in each window. Background wind fields, used to provide a first guess for the cold start cycle and boundary conditions for subsequent cycles, were generated using a velocity azimuth display (VAD; [Lhermitte and Atlas, 1961]), coupled with other available observations, as well as RUC model analyses. Once the background fields had been generated, the radar data were assimilated into the system.

Assimilation of the radar data was performed using a continuous cycling procedure [Sun and Crook, 2001]. As previously discussed in Section 2.3, an optimal fit between the model and the data was obtained by minimizing the difference between the model and observations (i.e., minimization of the cost function). This was accomplished by running (cycling) the numerical model forward and the adjoint of the model backward until an optimum solution was obtained. Model results (horizontal convergence at each pixel) were then saved as output grids. Mean BLC values at each horizontal grid-point were taken as the mean convergence within the lowest 1.5 km of the model domain (3 lowest model layers). Due to the length of the assimilation window, the VDRAS analysis resulted in an output grid for every other volume of radar data resulting in a total of 631 VDRAS output grids for use in this study.

3.3 Total Area Convergence (TAC) and Total Cell Convergence (TCC)

To quantify the overall magnitude of the boundary layer convergence occurring over a given area, the VDRAS convergence fields were used to compute the area-averaged convergence, or total-area convergence (TAC); given as the grid point mean convergence within an enclosed area [Cunning et al., 1982]. Equivalent to the negative of the line integral of the normal component of the wind around the area, this number provides a quantitative measure of the amount of horizontal mass flux into (positive values) or out of (negative values) an area, which can then be used to infer the relative magnitude and sign of compensating vertical motions.

Although TAC proves to be of utility when diagnosing horizontal mass flux in an *Eulerian* sense [e.g., Watson and Blanchard, 1984; Watson et al., 1987], and is an appropriate metric for the quantitative comparisons associated with the spatial climatologies to be presented in Section 4.1, this quantity is inappropriate for use in our cell-scale analyses where compensating areas of convergence/divergence within the BL associated with storm-scale

up/down drafts routinely coexist; here we are most concerned with sub-cloud forcing that acts to enhance upward vertical motions within the cell. Therefore, a more appropriate method of determining that portion of the flow capable of forcing upward motions within a cell would be to integrate the positive mean BLC values contained within the cell; we call this quantity total cell convergence (TCC) and will use it as our primary metric when discussing differences in VDRAS derived mean BLC between convective cells in Section 4.2.

3.4 Cell identification methodology

The datasets described above were used as input parameters into an IDL variant [as modified by Gauthier et al., 2010] of the Thunderstorm Identification, Tracking, Analysis and Nowcasting (TITAN) software [Dixon and Wiener, 1993] where individual cells were identified throughout the domain for the entire period of interest.

For the purpose of this study, a storm cell is defined as a contiguous region (2 or more pixels) of low level (z=2 km above ground level) radar reflectivity with values greater than or equal to 30 dBZ. Using geometric logic regarding storm cell positions and shapes, the algorithm identifies cells that occured within the domain of interest. Since pixel relative BLC, IM and FC measurements had previously been computed, cell totals of each parameter were taken as the sum of positive BLCs (justified in Section 3.3), IMs and FCs associated with each pixel comprising the cell; cell FDs were computed by normalizing the cell FC by cell area. As pointed out by Gauthier et al. [2010], this approach effectively treated each cell as a vertical entity, accounting for neither vertical tilt, nor ground flashes coming to ground in regions of reflectivity less than 30 dBZ.

4. Results and discussion

As previously outlined, the data gathered for this investigation were used to construct a spatial climatology of convergence over and around the Houston metropolitan area. Herein, we present results in the form of time-integrated analyses (Section 4.1) with the results of the cell-scale analyses presented separately in Section 4.2.

4.1 Time integrated analysis

Figure 2a presents the spatial distribution of VDRAS derived BLC (mean convergence within the lowest 1.5 km of the atmosphere) averaged over all hours contained within the 15-day dataset (note that only positive convergent flow is contoured in this figure). Consistent with the wind and convergence climatologies presented in Gauthier [*in-press*], a definite area of localized convergence over the Houston area is apparent in the 15-day mean. Relating the forcing produced by the BLC to the atmospheric response, Figure 2b presents a spatial composite with ground flash densities (FDEN; blue contours) and shaded contours of precipitation ice mass (IM) overlaid upon the VDRAS derived BLC presented in Figure 2a. From this presentation, a new link in the forcing-response chain begins to emerge. Here, we see that persistently focused, low-level, mesoscale forcing (on the order of 4-5 cm s^{-1}, computed based on continuity) over the Houston area, may give rise to a preferential location of convective initiation (CI), leading to downwind enhancements of radar derived precipitation ice mass within the charging zone (i.e., displaced from peak forcing), and

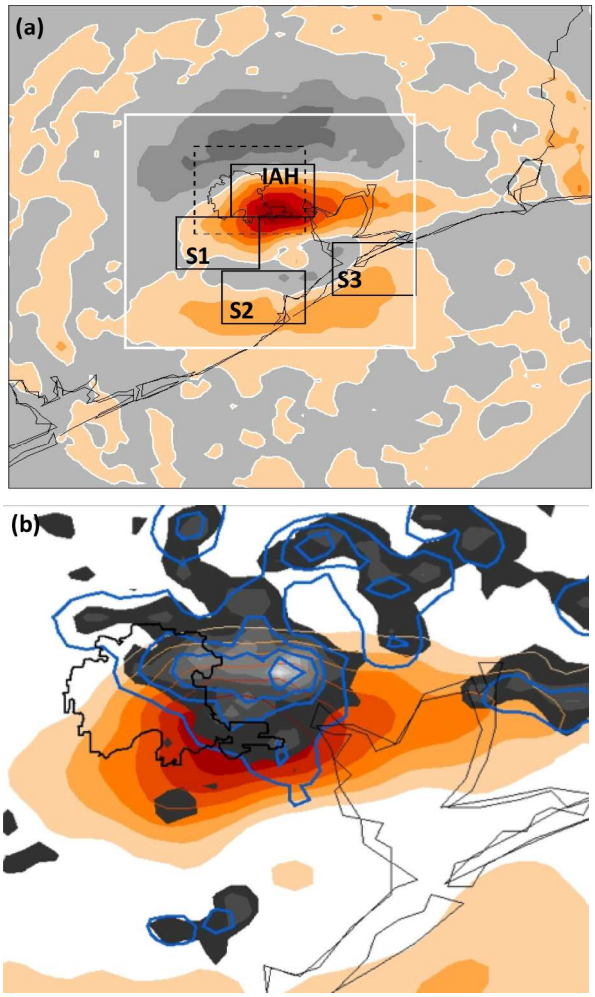

Fig. 2. Spatial distribution of the 15-day day time integrated mean (a) VDRAS derived boundary layer convergence (BLC) field with darkening shades of maroon associated with increasing positive convergence contoured at intervals of 1×10^{-5} sec^{-1}, relative to the zero value depicted by the white contour. Negative convergence (i.e., divergence) is represented by darkening shades of gray contoured at intervals of -1×10^{-5} sec^{-1}, relative to the same zero value contour, black reference boxes denote sub-domains discussed in the text, white box denotes that portion of the domain presented in Figure 2b; and (b) zoomed composite representation of normalized (relative to the domain maximum of each quantity) time integrated BLC (with shades of maroon increasing in darkness every 15%, beginning at 10% of the maximum BLC value within the domain, note divergent flow is not presented), radar derived precipitation ice mass (with shades of gray decreasing in intensity every 10%, beginning at 20%) and ground flash densities contoured in blue at the 20, 40, 60 and 80% levels, relative to the domain maximum flash density value associated with the 15-day mean.

finally enhancements in ground flash densities. Arguably, this sequence of events will, in and of itself, spawn localized (storm scale) regions of convergent and divergent flow serving to enhance and/or diminish the magnitude of the climatological convergence anomaly; however, the localized persistence of mesoscale BLC in the mean is consistent with the findings, and speculations contained in the aforementioned literature. Indeed, the persistent convergence located over the city is consistent with observations presented in Gauthier et al. [2010] where the authors found an area of enhanced composite cell merger occurrence located over and downwind of the city. The fact that the locations of enhanced convergence and cell merger activity are in general agreement further highlights the significance that cell mergers have with respect to convective intensity [Simpson, 1980; Simpson et al., 1980; Tao and Simpson, 1984].

Quantifying these spatial observations, Table 1 contains summary statistics of the spatial differences between the various sub-domains; statistics include daily mean values of TAC, IM and conditional FDEN (i.e., total flashes in each analysis box normalized by the area encompassing all pixels containing lightning) taken over all 15 days within our VDRAS subset. Clearly, relative to the other sub-domains, the Houston area (IAH) falls victim to enhanced forcing (TAC) leading to enhancements in PIM, and ultimately conditional FDENs. Comparison of the statistics associated with the remaining sub-domains (against one another) indicates that BLC alone, although an important ingredient, is not, in and of itself, sufficient to spawn deep moist convection and that meteorological conditions (i.e., the presence of sufficient moisture and instability) must be sufficient to allow this to occur. To illustrate this fact, we note that analysis boxes S2 and S3 have nearly equivalent values of TAC; however, the atmosphere responds more vigorously to the climatological forcing over S2 with greater enhancements in precipitation ice mass and resultant ground flash densities.

Analysis Box	Mean TAD [10^{-5} s^{-1}]	Mean IM [10^{7} kg km^{-2} day^{-1}]	Mean FDEN [10^{-3} flashes km^{-2} day^{-1}]
IAH	2.50	3.70	1.000
S1	0.94	1.80	0.200
S2	0.46	1.00	0.100
S3	0.45	0.51	0.027

Table 1. VDRAS summary statistics, see text for description.

Explanation for the dearth in lightning activity over the mouth of Galveston Bay (S3) can likely be found in the stabilizing effect that the cooler water temperatures have on the atmosphere. Although S2 (a coastal location) is also quite influenced by the Gulf waters, the stronger land-ocean contrasts likely serve to provide the necessary boost in instability enabling the enhanced response, relative to S3. Regardless of the reason for the subtle differences found within the climatological summary just presented, it is clear that the Houston area is more favorable for the development of deep moist convection resulting in enhanced ground flash densities relative to its immediate surroundings.

4.2 Cell scale analysis

Complementing the time integrated analyses just presented, all 631 convective radar volumes, along with accompanying VDRAS derived BLC fields, radar derived IMs and

NLDN detected CG lightning strikes were ingested into the modified cell tracking algorithm resulting in the identification of 1,928 lightning producing cells and 12,133 non-lightning producing cells throughout the domain; recall that the subjective definition of a cell is that of the area enclosed by the 30 dBZ radar reflectivity contour at 2 km above the ground. In this section we first discuss spatial differences between mean cell characteristics for cells geo-located in each of the sub-domains compared in Section 4.1 (IAH, S1, S2 and S3), we then go on to investigate differences between lightning and non-lightning cells in general, throughout the domain.

To that end, Table 2 provides a summary of the statistics to be discussed in this section. Focusing first on Table 2, columns a-d, we note that the IAH analysis box contained nearly 60% of the CG lightning producing cells (CG) observed in all analysis areas, and relative to the other sub-domains mean TCC associated with these cells were the greatest. Consistent with these findings we also note that the IAH CG cells contained larger quantities of precipitation ice mass located within the charging zone with higher CG flash rates (by a factor of 2, save S2). Comparing CG cells located within analysis boxes S1 and S2 (Table 2, columns b and c) , we note larger mean TCC values associated with S1 CG cells (mean values over twice that observed in S2); however, CG cells located within S2 contain 1.5 times as much IM and produce nearly 23% more lightning on a per cell basis. As in the previous section, the apparent discontinuity between the low-level forcing and the atmospheric response, lead us to conclude that relative to S1, analysis area S2 must be more favorable for the formation of deep moist convection, at least during the 15 days on which this analysis was based.

	(a) **IAH**		(b) **S1**		(c) **S2**		(d) **S3**		(e) **DOMAIN**	
	CG	noCG	CG	noCG	CG	noCG	CG	noCG	CG	noCG
COUNT	127	297	40	302	44	176	9	79	1,928	12,133
TCC [10^{-3} sec^{-1}]	1.80	0.29	1.10	0.30	0.50	0.30	0.36	0.12	1.60	0.23
IM [10^5 kg]	161	9	85	10	130	9	47	6	145	9
Flashes [per cell]	6.55		3.175		3.9		2.1		5.13	
FDEN [flashes km^{-2} $cell^{-1}$]	0.027		0.02		0.027		0.017		0.02	

Table 2. VDRAS summary statistics associated with 14,061 convective cells, see text for description.

Some insightful findings surrounding the characteristic differences between lightning and non-lightning (noCG) cells surface when comparing the mean statistics associated with all cells identified within the dataset (summarized in Table 2, column e). Here we see that, on average, CG cells have TCC values approximately 7 times greater than noCG cells with IM values being an order of magnitude larger. Not included in Table 2, we also note that the average peak radar reflectivity at tracking altitude (i.e., peak reflectivity at an altitude of 2 km) is on the order of 10 dBZ greater in the CG cells, nearly 50 dBZ.

The relationship between TCC, cell total IM and FDEN, is shown in Figure 3, where we present a three-parameter scatter plot of TCC and cell total IM, with varying pixel colors based on the flash density associated with the each particular cell. We first note a linear correlation (R = 0.7) between TCC and cell total IM with enhanced BL forcing associated with cells containing enhanced quantities of precipitation ice in the charging zone. Consistent with the findings of Gauthier et al. [2006], we further note that cells with more IM generally have larger ground flash densities associated with them (see dark gray and red data points in Figure 3). The fact that the most electrically intense storms (from a CG perspective) do not reside in the extreme upper-right hand portion of the parameter space is reassuring, as previous studies have highlighted an apparent anti-correlation between storms with extremely intense updrafts (> 30-35 m s^{-1}) and CG lightning production [e.g., MacGorman et al., 1989, Lang et al., 2000; Lang and Rutledge, 2002]. Hypothesized to be the result of an "elevated charge mechanism," it is argued that intense updrafts loft the main negative charge layer to greater altitudes than normal, thereby reducing the magnitude of the electric field between the main negative charge center and ground due to the increased spatial separation; this sequence of events would also likely delay the development of the lower positive charge center (LPCC) believed to be important in the development of ground flashes. It follows that this reduction in electric field may then favor intra-cloud (IC) lightning over CG lightning until such time as the storm begins to weaken, allowing the descent of precipitation ice to warmer regions of the cloud. This eventuality may then lead to the possible development of a the LPCC (recall discussions on the

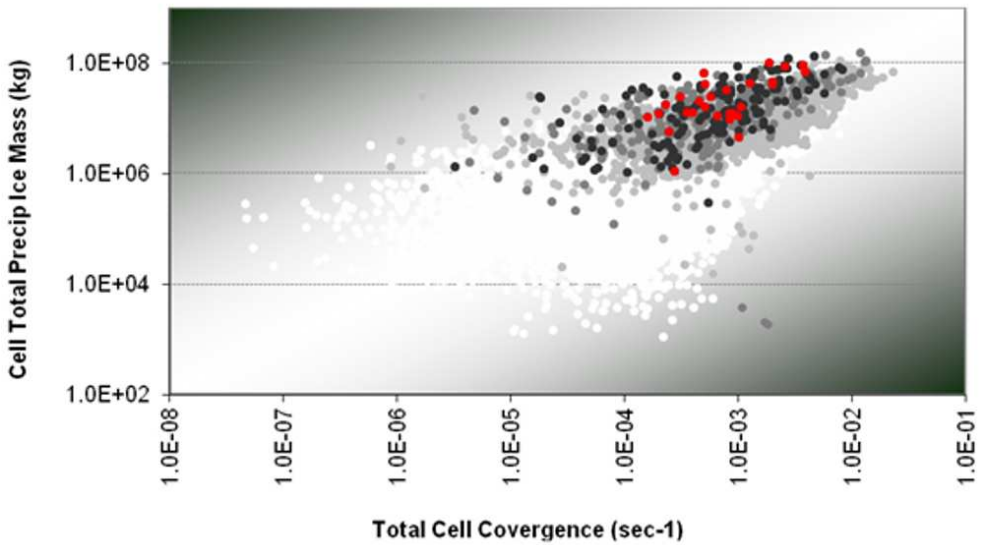

Fig. 3. A three-parameter scatter plot of cell total precipitation ice mass (IM; ordinate) as a function of total cell convergence (TCC; abscissa) and cell flash density (FDEN; no lightning = white, with increasing shades of gray associated with more intense flash densities, light gray = FDENs in the lower 3 quartiles of the conditional cumulative FDEN distribution, medium gray = FDEN within the 75-90th percentile range, dark gray = FDEN > 90th percentile with cells producing the most intense flash densities plotted in red).

development of the electrical tripole presented in Section 2.2) reinvigorating the occurrence of CG flashes. Although unable to quantify it, we suspect that this is what we are observing in Figure 3, where strong updraft enhancements (on the order of 15-25 m/s, based on convergence alone) are associated with a decrease in ground flash densities of storms that have been electrically "primed" (i.e., storms containing ample precipitation sized ice particles in the mixed-phase region).

5. Conclusion

Utilizing BL convergence fields generated by NCAR's Variational Doppler Radar Assimilation System, we investigated the relationship between VDRAS derived boundary layer convergence, radar derived precipitation ice mass and NLDN detected CG lightning over 15 non-consecutive summer days, independently establishing the presence of an enhanced convergence zone located in the vicinity of the Houston metropolitan area. Coupling *Eulerian* and cell-scale analyses over the Houston area, we clearly link the BL convergence zone with enhancements in radar derived precipitation ice mass and ultimately enhanced ground flash densities. Statistics associated with over 14,000 convective cells occurring throughout the domain highlight distinct differences between lightning and non-lightning producing cells, with the average lightning producing cells having convergence based updraft enhancements nearly 7 times that of non-lightning producing cells, with an order of magnitude increase in precipitation ice mass within the charging zone. Collectively, the findings presented in this chapter firmly establish a physical proportionality between the ability of the cloud ensemble to produce enhanced CG lightning activity, and the amount of low-level convergent flow available to feed the updraft(s).

6. Acknowledgment

This research was supported by funding from the U.S. Air Force Academy through the Air Force Institute of Technology. Special thanks go to Dr. Andrew Crook and his staff at NCAR for their assistance and expertise in running the VDRAS analyses used in this study, without their efforts this project would not have been possible. The views expressed in this paper are those of the author and do not reflect the official policy or position of the U.S. Air Force, Department of Defense, or the U.S. Government.

7. References

Banacos, P. C., and D. M. Schultz (2005). The use of moisture flux convergence in orecasting convective initiation: Historical and operational perspectives, *Weather and Forecasting*, 20(3), 351-366.

Battan L. J. (1965). Some factors governing precipitation and lightning from convective clouds, *Journal of Atmospheric Science, 22,* 79-84.

Crook N. A., and J. Sun (2004). Analysis and forecasting of the low-level wind during the Sydney 2000 Forecast Demonstration Project, *Weather and Forecasting., 19,* 151-167.

Cummins, K. L., M. J. Murphy, E. A. Bardo, W. L. Hiscox, R. B. Pyle, and A. E. Pifer (1998). A combined TOA/MDF technology upgrade of the U.S. National

Lightning Detection Network, *Journal of Geophysical Research, 103*(D8), doi: 10.1029/98JD00153.

Cunning J. B., R. L. Holle, P. T. Gannon, and A. I. Watson (1982). Convective evolution and merger in the FACE experimental area: Mesoscale convection and boundary layer interactions, *Journal of Applied Meteorology, 21,* 953-977.

Dixon, M., and G. Wiener (1993). TITAN: thunderstorm identification, tracking, analysis, and nowcasting—A radar-based methodology, *Journal of Atmospheric and Oceanic Technology, 10*, 785-797.

Gauthier, M. L., W. A. Petersen, L. D. Carey, and R. E. Orville (2005). Dissecting the anomaly: A closer look at the documented urban enhancement in summer season ground flash densities in and around the Houston area, *Geophysical Research Letters, 32,* L10810, doi:10.1029/2005GL022725.

Gauthier, M.L., Petersen, W.A., Carey, L.D., Christian, H.J. (2006). Relationship between cloud-to-ground lightning and precipitation ice mass: a radar study over Houston. *Geophysical Research Letters,* 33, L20803. doi:10.1029/2006GL027244.

Gauthier, M. L., Petersen, W. A., Carey, L. D. (2010). Cell mergers and their impact on cloud to-ground lightning over the Houston area. *Journal of Atmospheric Research,* doi: 10.1016/j.atmosres.2010.02.010.

Gauthier, M. L. (*in-press*). Investigating possible causative mechanisms behind the Houston cloud-to-ground lightning anomaly, In: *Climatology: New Developments,* A. Herveoux, E. Suthland, Nova Science Publishers, Inc., ISBN: 978-1-62100-322-9, Hauppauge, New York.

Jayaratne, E. R., C. P. R. Saunders, and J. Hallet (1983). Laboratory studies of the charging of soft hail during ice crystal interactions, *Quarterly Journal of the Royal Meteorological Society, 109*, 609-630.

Lang, T. J., and S. A. Rutledge (2002). Relationships between convective storm kinematics, precipitation, and lightning, *Monthly Weather Review, 130,* 2492-2506.

Lang, T. J., S. A. Rutledge, J. E. Dye, M. Venticinque, P. Laroche, and E. Defer (2000). Anomalously low negative cloud-to-ground lightning flash rates in intense convective storms observed during STERAO-A. *Monthly Weather Review, 128,* 160-173.

Lhermitte, R. M., and D. Atlas (1961). Precipitation motion by pulse Doppler, *Proc. Ninth Weather Radar Conf.,* Kansas City, MO, American Meteorological Society, 218–223.

MacGorman, D. R., D. W. Burgess, V. Mazur, W. D. Rust, W. L. Taylor, and B. C. Johnson (1989). Lightning rates relative to tornadic storm evolution on 22 May 1981, *Journal of Atmospheric Science, 46*, 221-250.

Orville, R. E., G. Huffines, J. Nielsen-Gammon, R. Zhang, B. Ely, S. Steiger, S. Phillips, S. Allen, and W. Read (2001). Enhancement of cloud-to-ground lightning over Houston, Texas, *Geophysical Research Letters, 28*(13), doi:10.1029/2001GL012990.

OTD Global Lightning Image obtained from http://thunder.msfc.nasa.gov/otd/ maintained by NASA EOSDIS Global Hydrology Resource Center (GHRC) DAAC, Huntsville, AL. 2011. Data for the image were provided by the NASA EOSDIS GHRC DAAC.

Petersen, W. A., H. J. Christian, and S. A. Rutledge (2005). TRMM observations of the global relationship between ice water content and lightning, *Geophysical Researhc Letters, 32,* L14819, doi:10.1029/2005GL023236.

Saunders, C. P. R., W. D. Keith, and R. P. Mitzeva (1991). The effect of liquid water on thunderstorm charging, *Journal of Geophysical Reasearch, 96,* 11,007-11,017.

Simpson, J. (1980). Downdrafts as linkages in dynamic cumulus seeding effects, *Journal of Applied Meteorology, 19,*477-487.

Simpson, J. N. E. Westcott, R. J. Clerman, and R. A. Pielke (1980). On cumulus mergers, *Arch. Met. Geoph. Biokl., 29*, 1-40.

Steiger S. M., R. E. Orville, and G. Huffines (2002). Cloud-to-ground lightning characteristics over Houston, Texas: 1989-2000, *Journal of Geophyical Reserearch, 107*(D11), doi:10.1029/2001JD001142.

Sun J., and N. A. Crook (1997). Dynamical and microphysical retrieval from doppler radar observations using a cloud model and its adjoint. Part I: Model development and simulated data experiments, *Journal of Atmospheric Science, 54(12),* 1642-1661.

Sun J., and N. A. Crook (1998). Dynamical and microphysical retrieval from doppler radar observations using a cloud model and its adjoint. Part II: Retrieval experiments of an observed Florida convective storm, *Journal of Atmospheric Science, 55(5),* 835-852.

Sun, J., and N. A. Crook (2001). Real-time low-level wind and temperature analysis using single WSR-88D data, *Weather and Forecasting, 16(1)*, 117-132.

Takahashi, T. (1978), Rimin g electrification as a charge generation mechanism in thunderstorms, *Journal of Atmospheric Science, 35*, 1536-1548.

Tao, W.-K., and J. Simpson (1984). Cloud interactions and merging: Numerical simulations, *Journal of Atmospheric Science, 41,* 2901-2917.

Ulanski S. L., and M. Garstang (1978). The role of surface divergence and vorticity in the life cycle of convective rainfall. Part I: Observation and analysis, *Journal of Atmospheric Science, 35,* 1047-1062.

Wacker, R. S., and R. E. Orville (1999a). Changes in measured lightning flash count and return stroke peak current after the 1994 U.S. National Lightning Detection Network upgrade: 1. Observations, *Journal of Geophysical Research, 104*(D2), doi:10.1029/1998JD200060.

Wacker, R. S., and R. E. Orville (1999b). Changes in measured lightning flash count and return stroke peak current after the 1994 U.S. National Lightning Detection Network upgrade: 2. Theory, *Journal of Geophysical Research, 104*(D2), doi:10.1029/1998JD200059.

Watson A. I., and D. O. Blanchard (1984). The relationship between total area divergence and convective precipitation in South Florida, *Monthly Weather Review, 112,* 673-685.

Watson A. I., R. E. López, R. L. Holle, and J. R. Daugherty (1987). The relationship of lightning to surface convergence at Kennedy Space Center: A preliminary study, *Weather and Forecasting, 2,* 140-157.

Westcott, N. E. (1995). Summer-time cloud-to-ground lightning activity around major Midwestern urban areas, *Journal of Applied Meteorology, 34*, 133-1642.

Williams, E. R. (1989). The tripole structure of thunderstorms, *Journal of Geophysical Research*, *94*, 13,151-13,167.

Workman, E. J., and S. E. Reynolds (1949). Electrical activity as related to thunderstorm cell growth, *Buletin of the American Meteorological Society*, *30*, 142-149.

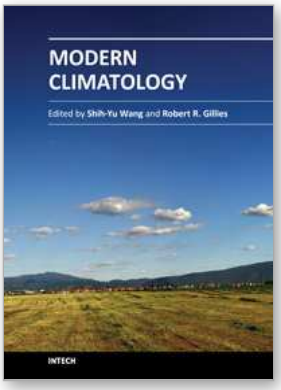

Modern Climatology

Edited by Dr Shih-Yu Wang

ISBN 978-953-51-0095-9
Hard cover, 398 pages
Publisher InTech
Published online 09, March, 2012
Published in print edition March, 2012

Climatology, the study of climate, is no longer regarded as a single discipline that treats climate as something that fluctuates only within the unchanging boundaries described by historical statistics. The field has recognized that climate is something that changes continually under the influence of physical and biological forces and so, cannot be understood in isolation but rather, is one that includes diverse scientific disciplines that play their role in understanding a highly complex coupled "whole system" that is the earth's climate. The modern era of climatology is echoed in this book. On the one hand it offers a broad synoptic perspective but also considers the regional standpoint, as it is this that affects what people need from climatology. Aspects on the topic of climate change - what is often considered a contradiction in terms - is also addressed. It is all too evident these days that what recent work in climatology has revealed carries profound implications for economic and social policy; it is with these in mind that the final chapters consider acumens as to the application of what has been learned to date.

How to reference

In order to correctly reference this scholarly work, feel free to copy and paste the following:

Michael L. Gauthier (2012). On the Relationship Between Boundary Layer Convergence and Cloud-to-Ground Lightning, Modern Climatology, Dr Shih-Yu Wang (Ed.), ISBN: 978-953-51-0095-9, InTech, Available from: http://www.intechopen.com/books/modern-climatology/on-the-relationship-between-boundary-layer-convergence-and-cloud-to-ground-lightning

INTECH
open science | open minds

InTech Europe
University Campus STeP Ri
Slavka Krautzeka 83/A
51000 Rijeka, Croatia
Phone: +385 (51) 770 447
Fax: +385 (51) 686 166
www.intechopen.com

InTech China
Unit 405, Office Block, Hotel Equatorial Shanghai
No.65, Yan An Road (West), Shanghai, 200040, China
中国上海市延安西路65号上海国际贵都大饭店办公楼405单元
Phone: +86-21-62489820
Fax: +86-21-62489821